

# Spin-selective transport through Fe/AlO<sub>x</sub>/GaAs(100) interfaces under optical spin orientation

T. Taniyama,\* G. Wastlbauer, A. Ionescu, M. Tselepi, and J. A. C. Bland†

*Cavendish Laboratory, University of Cambridge, Madingley Road, Cambridge CB3 0HE, United Kingdom*

(Received 7 March 2003; revised manuscript received 23 May 2003; published 17 October 2003)

Spin-selective transport of optically excited polarized electrons through Fe/GaAs(100) and Fe/AlO<sub>x</sub>/GaAs(100) interfaces is reported. A visible enhancement in the spin selectivity is observed in the Fe/AlO<sub>x</sub>/GaAs(100) structure at a forward bias of 0.04 V, while no such feature is seen in the Fe/GaAs(100) structure. The spin selectivity in the Fe/AlO<sub>x</sub>/GaAs(100) structure has a maximum value which is a factor of 2 larger than that of the Fe/GaAs(100) structure at the same bias of 0.04 V. The effect can be understood in terms of the spin dependent tunneling of electrons through the oxide barrier in the Fe/AlO<sub>x</sub>/GaAs(100) structure, while its clear bias dependence excludes magnetic circular dichroism as a possible mechanism.

DOI: 10.1103/PhysRevB.68.134430

PACS number(s): 75.70.-i, 72.25.Mk, 72.25.Fe, 85.75.-d

## I. INTRODUCTION

The exploration of spin transport through ferromagnetic metal (FM)/ semiconductor (SC) interfaces is rapidly leading toward innovations in spin engineering, e.g., spin transistors or quantum computation.<sup>1,2</sup> For successful device applications, realizing high efficiencies of spin injection and spin selection through interfaces is of decisive importance. Many researchers have reported spin injection from FM into SC materials, detecting the polarization of light emitted via the recombination of electrons and holes in the SC.<sup>3-11</sup> The circular polarization values reported, however, have varied from 0.5% at room temperature<sup>10</sup> to 4% at 240 K even with the same choice of metal Fe. On the other hand, spin selection at the FM/SC interface, which is regarded as the opposite effect of the spin injection, has been examined by only a few groups for some particular interfaces, i.e., Co/Al<sub>2</sub>O<sub>3</sub>/*p*-GaAs and NiFe/GaAs.<sup>12-15</sup> The principal idea relies on the asymmetry of the transmission for each spin channel through the FM layer.<sup>16,17</sup> Electrons in the SC with spin orientation parallel to the FM are easily transmitted through the high-conductivity spin channel while those with the antiparallel spin orientation are blocked at the interface. The fundamental transport process of the electrons at the interface, i.e., diffusive transport, ballistic transport or tunneling, drastically changes the efficiencies of the two effects.<sup>18</sup> In the diffusive process, the spin selection is significantly suppressed due to spin-flip processes at the interface whereas no spin flip occurs in ballistic and tunneling processes, leading to the efficient selection of a preferable spin orientation. Therefore, modifying the electronic states at the interface should provide a means of obtaining crucial information on achieving high efficiencies of spin injection and spin selection: to date the role of the interface is still elusive.

In this paper, we report on the spin-selective transport of electrons through contrasting Fe/GaAs(100) and Fe/AlO<sub>x</sub>/GaAs(100) interfaces using optical spin orientation in GaAs (Fig. 1). Irradiation by circularly polarized light excites interband transitions from  $P_{3/2}$  and  $P_{1/2}$  to  $S_{1/2}$  at the  $\Gamma$  point of GaAs, for which the transition selection rule yields electrons with a maximum spin polarization of 50% in GaAs.<sup>19</sup> We find an enhancement in the photocurrent asym-

metry defined by the helicity of the incident light at a forward bias in the Fe/AlO<sub>x</sub>/GaAs(100) devices. As a result, a maximum occurs in the photocurrent asymmetry at forward bias, whereas no such maximum appears in the Fe/GaAs(100) structure. This result clearly demonstrates spin-selective transport due to tunneling through the interface.

## II. EXPERIMENTAL PROCEDURE

Fe layers with a thickness of 3 nm were deposited in an ultrahigh vacuum chamber  $\sim 10^{-10}$  mbar on AlO<sub>x</sub>(5 nm)/*n*GaAs(100) (Si:  $1 \times 10^{18}$  cm<sup>-3</sup>), where Al layers were first deposited in a different low vacuum chamber and naturally oxidized. Before depositing Fe layers, the

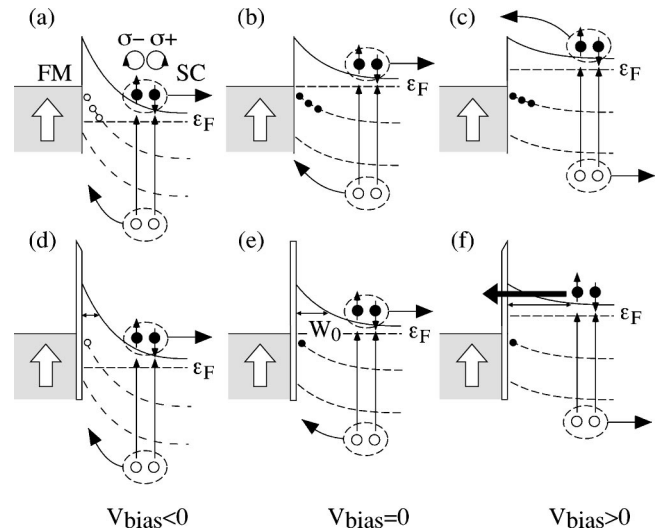


FIG. 1. Schematic diagram of principal carrier transport process at FM/SC and FM/AlO<sub>x</sub>/SC interfaces under laser irradiation. (b) and (e) illustrate the electronic structures at zero bias for FM/SC and FM/AlO<sub>x</sub>/SC interfaces, respectively. At reverse bias, (a) and (d), excited electrons flow into the GaAs bulk while holes are collected into the Fe layer. At forward bias, excited electrons in the FM/SC flow over the Schottky barrier (c), whereas those in the FM/AlO<sub>x</sub>/SC transmit through the barrier via the tunneling process (f). Electrons and holes are represented by the large closed and open circles, respectively. Recombination centers are represented by the small closed and open circles in the vicinity of the interface.

$\text{AlO}_x$  layers were sputtered with Ar plasma and annealed at  $500^\circ\text{C}$  to attain flat surfaces. The typical results for the samples (1) Fe(3nm)/GaAs(100), (2-a) Fe(3 nm)/ $\text{AlO}_x$ (5 nm)/GaAs(100), and (2-b) Fe(3 nm)/ $\text{AlO}_x$ (5 nm)/GaAs(100) are examined hereafter. Low energy electron diffraction observation revealed that the Fe layer of the sample (1) was grown epitaxially and those of the samples (2-a) and (2-b) were polycrystalline. The photocurrent  $I_{ph}$  induced by the front irradiation at wavelength  $\lambda = 633$  nm (1.96 eV photon energy) was measured from the voltage drop across an external load resistor in a closed circuit.<sup>14</sup> We also measured the spin polarized photocurrent  $I_+$  ( $I_-$ ) excited by the right- (left-) handed circularly polarized light, and the difference ( $\Delta I_{heli} = I_+ - I_-$ ) between the photocurrents was collected by means of a photoelastic modulator (PEM) at room temperature.<sup>14</sup> All the photocurrent measurements were performed using a lock-in technique, which enables us to extract the current excited by the irradiation efficiently even though there is a significant dark current. Contacts for the electrical measurements were made using a planar electrode geometry—see inset of Fig. 2.

### III. RESULTS

#### A. Sample characterization

As the magnitude of spin dependent transport strongly depends on the morphology of the interface, we used first transmission electron microscopy to observe cross sections of the samples to check whether there is any morphological difference between the samples. The transmission electron microscopy shows that the  $\text{AlO}_x$  layer of sample (2-a) has a rough morphology compared with sample (2-b). The morphological difference also influences the magnetization processes of the samples. The magnetization curves were obtained by polar magneto-optical Kerr effect (MOKE) measurements—solid lines in Fig. 4. In the film thickness regime of this study, the shape anisotropy dominates the magnetization process and the roughness of the ferromagnetic layer should reduce the anisotropy. The MOKE results are compatible with the degree of the roughness: the largest shape anisotropy is obtained in the epitaxial Fe layer [sample (1)] and introduction of the  $\text{AlO}_x$  layer suppresses the anisotropy. One may ask whether, when in proximity with an  $\text{AlO}_x$  layer, the Fe layer is stable against the formation of Fe oxide. In general, Al oxide is quite stable and unlikely to react with Fe unless a special Al oxidation process is employed. A previous report on tunnel junctions also supports this view.<sup>20</sup> The authors used reactive deposition of the Al oxide layer, in which Al was deposited on an Fe substrate in an oxygen atmosphere. Even in these conditions, the underlying Fe layer is stable against reaction with oxygen at the  $\text{AlO}_x$ /Fe interface. In our experiments, Fe layers were just deposited on the  $\text{AlO}_x$  layer in UHV at room temperature, thus indicating that the Fe layer is not likely to be oxidized by reacting with  $\text{AlO}_x$ .

It should also be noted that an Al layer of 5 nm may be too thick to be fully oxidized naturally due to a self-limiting mechanism of natural oxidation, indicating that an Al layer

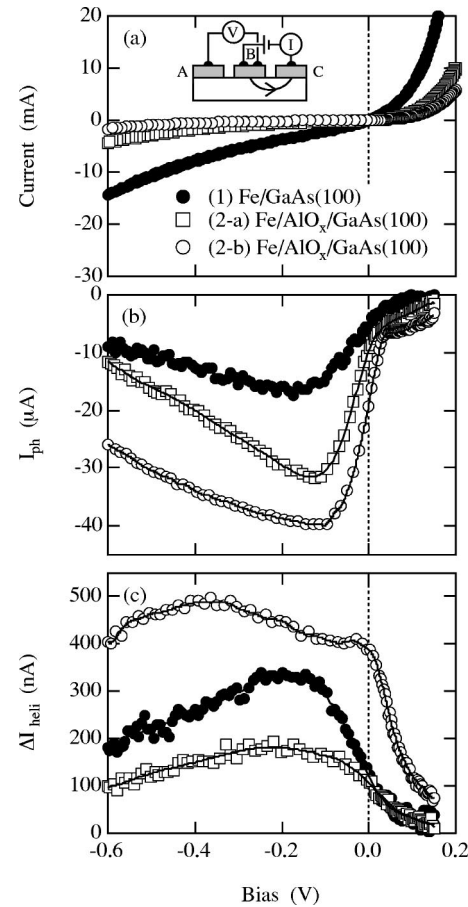


FIG. 2. (a)  $I(V)$  curves, (b) photocurrents  $I_{ph}$ , and (c) difference between the photocurrents excited with right- and left-circularly polarized lights  $\Delta I_{heli} = I_+ - I_-$  measured in 2 T perpendicular to the film plane as a function of bias voltage. The inset shows the planar contact geometry used for electrical measurements, which enables us to probe the voltage drop at the interface under the middle contact  $B$  only, so excluding the voltage drop associated with the electrical current flowing through the bulk of the GaAs substrate between contacts  $B$  and  $C$  (indicated by the arrow).

could remain between the GaAs substrate and the  $\text{AlO}_x$  layer. If this is the case, an AlGaAs layer can form at the interface by the diffusion of residual Al in the GaAs substrate during the annealing process at  $500^\circ\text{C}$ . This may also contribute to the quantitative differences in the  $\Delta I_{heli}$  seen for these samples, and probably can also account for the differing Schottky characteristics.

#### B. Current-voltage characteristics

As we have stated, the morphology of the interface greatly influences the current-voltage  $I(V)$  characteristics as shown in Fig. 2(a). Although all the samples show rectification due to the Schottky barrier, the leakage current at reverse bias is pronounced for the epitaxially grown sample (1). The poor Schottky characteristic could be caused by the Ga-rich GaAs(100) surface due to the sublimation of As ions during the annealing process at  $500^\circ\text{C}$ .<sup>21</sup> For the samples (2-a) and (2-b), on the other hand,  $\text{AlO}_x$  layers prevent the

sublimation, giving less leakage current for reverse bias. We attribute the difference in the  $I(V)$  curves between samples (2-a) and (2-b) to the morphology of the  $\text{AlO}_x$  layer: the flatter  $\text{AlO}_x$  interface of samples (2-b) provides the better rectification in Fig. 2(a).

### C. Photoexcited electron transport

The photocurrents  $I_{ph}$  as a function of bias voltage at the interface are shown in Fig. 2(b). A negative photocurrent is the typical characteristic of the metal-semiconductor diode with the band curvature in the depletion region of the semiconductor. The excited electrons in the GaAs near the interface flow into the GaAs bulk while simultaneously excited holes are collected in the Fe layers. The  $I_{ph}$  shows a broad peak at a reverse bias ( $\sim 0.15$  V) and decreases with greater reverse bias. The feature can be interpreted in terms of recombination at the interface as shown in Fig. 1. If the recombination centers are located just below the Fermi level at zero bias, the Fermi level goes across the energy levels of the recombination centers with increasing reverse bias, thereby electrons are released from the recombination centers. The positively charged recombination centers trap electrons from the Fe layer and holes excited by the light irradiation simultaneously. The release and trap processes effectively suppress the photocurrent. The tunneling of electrons directly from the Fe layer into the positively charged recombination centers also contributes to the dark current at reverse bias. These processes occur in both the structures with or without the  $\text{AlO}_x$  layer. Assuming that the recombination centers are associated with the defects created in the annealing process, the capture cross sections for electrons and holes are expected to be larger in the sample (1) due to the sublimation of As. The description consistently explains the  $I(V)$  characteristics in which the sample (1) exhibits the significant leakage current at reverse bias.

Another prominent feature is a dip of the photocurrent at 0.04 V for the samples (2-a) and (2-b). Both the excited electrons and holes could contribute to the photocurrent in our samples. The photocurrent due to the holes, however, should not give the anomaly at forward bias as the electronic structure of the recombination centers, which are trapping electrons, does not change with the bias. This indicates that the dip is associated with the transport of excited electrons through the interface from the GaAs to the ferromagnetic Fe. The excited electrons pass through the interface via thermally assisted transport over the Schottky and/or the  $\text{AlO}_x$  insulating barrier and the tunneling through the barriers. The transmission of electrons due to the thermally assisted transport is determined by the height of the barrier, but that due to the tunneling depends on a combination of height and width. The effective height of the Schottky barrier is reduced with increasing forward bias whereas the barrier width increases, suggesting that there exists an optimum bias for the electrons to tunnel through the barrier. In this sense, the tunneling of the excited electrons through the barrier is most likely to occur at a forward bias value determined by the subtle balance between the barrier height and width, thus causing the dip of the photocurrent as we observe.

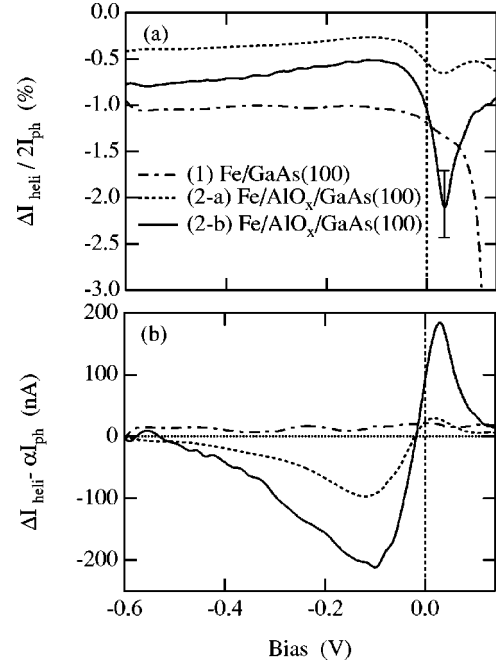


FIG. 3. (a) Bias dependence of  $\Delta I_{heli}/2I_{ph}$  of the samples (1), (2-a), and (2-b). The magnitude of the error in this quantity for sample (2-b) is indicated by a single representative errorbar for the point at 0.04 V. (b) Bias dependence of the effective spin-selective photocurrent contribution  $\Delta I_{heli} - \alpha I_{ph}$  for the samples (1), (2-a), and (2-b).

### D. Spin selectivity of photoexcited electron transport

Figure 2(c) depicts  $\Delta I_{heli}$  in a field of 2 T sufficient to almost saturate the Fe film perpendicularly to the film plane. The  $\Delta I_{heli}$  of sample (1) exhibits a single peak at around  $-0.15$  V, which is quite similar to the bias dependence of the photocurrent shown in Fig. 2(b). On the other hand, the  $\Delta I_{heli}$  of sample (2-b) has a broad maximum at  $-0.38$  V and a shoulder at zero bias, being distinct from the corresponding  $I_{ph}$ . The sample (2-a) also shows different bias dependences between  $\Delta I_{heli}$  and  $I_{ph}$  as clearly shown in Fig. 3(b). The relative spin orientation of the excited electrons in GaAs and the out-of-plane Fe moments alters from parallel to antiparallel upon changing the helicity of the light irradiated on the GaAs. This means that the  $\Delta I_{heli}$  is attributed to the difference in the conductivities with spin-up and spin-down electrons with respect to the Fe moments: we term this spin selectivity. For a quantitative comparison between the different samples, the  $\Delta I_{heli}$  normalized by the corresponding photocurrent ( $\Delta I_{heli}/2I_{ph}$ ) is used, as  $\Delta I_{heli}$  increases proportionally with the number of excited electrons, i.e., the photocurrent. Figure 3(a) shows  $\Delta I_{heli}/2I_{ph}$  as a function of bias voltage at 2 T. To calculate  $\Delta I_{heli}/2I_{ph}$  precisely, the values for both  $\Delta I_{heli}$  and  $2I_{ph}$  were estimated at the same bias voltage by first fitting the data of Fig. 2 to smooth curves (solid curves in Fig. 2) and using interpolation. The sharp drop for sample (1) at  $\sim 0.12$  V is an extrinsic effect due to the vanishing photocurrent  $I_{ph}$  at around  $V_b$ . Of particular importance is the peak in  $\Delta I_{heli}/2I_{ph}$  at 0.04 V for the sample (2-a) and (2-b), which is obviously reflected by the dip in the photocurrent which occurs at 0.04 V and the shoul-

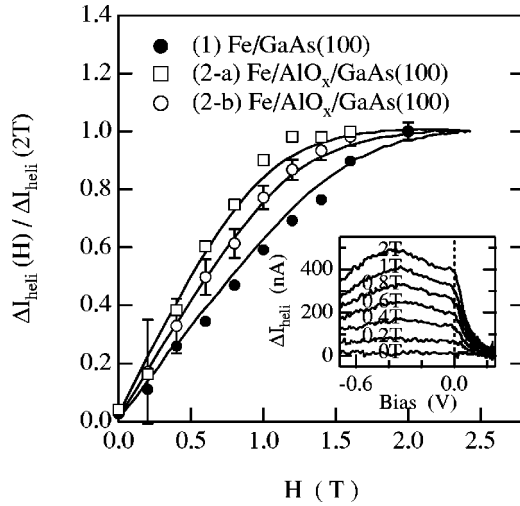


FIG. 4. Field dependence of  $\Delta I_{heli}$  normalized by the values in 2 T at zero bias. The solid lines are the magnetization curves obtained by polar magneto-optical Kerr effect measurements. The inset shows bias dependent  $\Delta I_{heli}$  of the sample (2-b) in various magnetic fields.

der in  $\Delta I_{heli}$  above zero bias, both of which are due to the tunneling process. The absence of the peak for the sample (1) is due to the poor Schottky barrier which makes electrons pass over the barrier rather than tunnel. Therefore, we conclude that the peak in  $\Delta I_{heli}/2I_{ph}$  at 0.04 V is a direct evidence that efficient spin-selective transport occurs due to the tunneling process at the interface in the presence of a tunneling barrier.

#### IV. DISCUSSION

The field dependence of  $\Delta I_{heli}$  obtained at zero bias further corroborates our description of the spin selectivity (Fig. 4). The  $\Delta I_{heli}$  values of the sample (1) hardly saturates even at 2 T while those of samples (2-a) and (2-b) saturate at 1.2 T and 1.6 T, respectively. Since  $\Delta I_{heli}$  should be proportional to the out-of-plane magnetization of the Fe layer, which is parallel or antiparallel to the spin of the excited electrons, the field dependence of  $\Delta I_{heli}$  is directly associated with the magnetization curve of the Fe layer. Indeed, the magnetization curves obtained by MOKE measurements well agree with the field dependence of  $\Delta I_{heli}$ . In addition, the magnitude of  $\Delta I_{heli}/2I_{ph}$  at reverse bias increases with increasing saturation field (see Fig. 4). This also can be understood from a consideration of the roughness of the film, which induces a magnetically inactive Fe component in the samples (2-a) and (2-b) due to thermal instability of the interface layers.

Magnetic circular dichroism (MCD) due to the Fe layer also might mimic the asymmetry of the photocurrent  $\Delta I_{heli}$ . The contribution of the MCD was estimated to be  $\sim 2.5\%$  for a 20-nm-thick Fe film by photoluminescence measurements,<sup>10</sup> which is in good agreement with the calculation for the Fe film.<sup>14</sup> A corresponding value of 0.4% is estimated for the MCD contribution in our 3-nm-thick Fe films, and an effective value for  $\Delta I_{heli}/2I_{ph}$  of 1.7% is estimated for the sample (2-b) at 0.04 V (the total measured

value is 2.1%). The effective value is comparable to the spin injection efficiency of 2% reported by Zhu *et al.*<sup>3</sup> Furthermore, if the spin selectivity is due to the MCD, the same bias dependences should be obtained for  $I_{ph}$  and  $\Delta I_{heli}$ : the bias dependences of Figs. 2(b) and 2(c) are clearly distinct, and so the MCD cannot explain the peak in the bias dependence of the  $\Delta I_{heli}/2I_{ph}$ . More explicitly, we can obtain a pure spin-selective contribution to the helicity dependent photocurrent by considering the fact that  $\Delta I_{heli}$  is a superposition of a MCD contribution and a pure spin-selectivity effect. Since the MCD contribution is proportional to the photocurrent  $I_{ph}$ , so the quantity  $\Delta I_{heli} - \alpha I_{ph}$  gives the pure spin selective contribution and consequently the MCD effect is subtracted. The values of  $\Delta I_{heli} - \alpha I_{ph}$  are shown in Fig. 3(b) as a function of bias voltage. The parameter  $\alpha$  is chosen so that  $\Delta I_{heli} - \alpha I_{ph}$  has a value of zero at  $-0.6$  V. The curves for the samples (2-a) and (2-b) clearly show a peak at 0.02 and 0.04 V, respectively, while the values for sample (1) remain almost the same over the bias range. Thus, we see qualitatively the same behavior in two separate samples in spite of the differing magnitude of the spin selectivity, i.e., qualitatively reproducible.

The MCD effect might significantly contribute to the spin selectivity at reverse bias because the spin lifetime of holes, which predominantly contribute to the photocurrent, is quite short. At forward bias, on the other hand, electron transport is becoming significant, which means that the peak in the spin selectivity in Fig. 3(a) has its origin in electron transport which has a longer spin lifetime. The interface effect should not increase the MCD because the magnetic moments of Fe at the  $\text{AlO}_x$  interface are likely to be reduced,<sup>22</sup> indicating that the MCD at the interface effect is reduced. Also the very small number of accumulated carriers at the interface is not likely to modify the MCD effect, since the change of the magnetization due to the accumulation is negligible compared with the magnetization of Fe layer. On the basis of these considerations, the peak in the spin selectivity in Fig. 3 is due to spin polarized electron tunneling from GaAs into Fe layer.

As a further check, we test whether we can obtain spin selectivity of spin polarized electron transport using a structure with a well-defined AlGaAs barrier instead of an  $\text{AlO}_x$  barrier layer.<sup>23</sup> While the  $\Delta I_{heli}$  shows a distinct bias dependences as the corresponding  $I_{ph}$  at low temperatures, the difference between the bias dependences of  $\Delta I_{heli}$  and  $I_{ph}$  becomes less pronounced with increasing temperature. Also the spin selectivity of the sample shows a peak at a forward bias that is similar to the present results for the samples with an  $\text{AlO}_x$  layer, and the value of the spin selectivity reduces with increasing temperature. Since the thermally assisted transport over the barrier is suppressed at low temperatures, this observation indicates that only the tunneling electrons show a significant spin dependent transport across the interface, in good agreement with our description of the spin dependent transport across a tunnel barrier for the  $\text{Fe}/\text{AlO}_x/\text{GaAs}(100)$  structure. Therefore, we believe that the enhancement in the  $\Delta I_{heli}/2I_{ph}$  is a clear manifestation of spin-selective transport at the interface.

A contribution of the excitation from the split-off band is

also included for the optical pumping with the photon energy of 1.96 eV we use, so that the spin polarization of the excited electrons is reduced to around 10%, although our previous measurements of the wavelength-dependent spin transport confirmed that optically excited electrons in GaAs with this energy were spin polarized.<sup>14</sup> It should also be noted that photoexcited electron transport includes both thermionic emission and tunneling contributions, indicating that the photoexcited current is not equal to the tunneling current. Therefore, the effective spin selectivity, which is defined to be the helicity dependent photocurrent normalized by the corresponding photocurrent, is artificially small. These considerations suggest that the spin selectivity obtained in this study is at a minimum, thus enabling us to expect a higher value of spin selectivity by optimizing the interface between GaAs and ferromagnetic metal.

Although the effects of a possible frequency-dependent phase shift should be considered, we have checked this in other experiments using a 1/4 wavelength plate,<sup>14</sup> the results of which broadly agree with the results obtained using a PEM. Also, the photocurrent measured by a PEM is not exactly the same as that measured at the optical chopping frequency. However, even the use of a PEM does not change the qualitative behavior or the relative magnitude of the he-

licity dependent effect measured when comparing samples. Therefore, the comparison between the samples is still valid.

## V. CONCLUSION

We demonstrate spin-selective electron transport at the Fe/AlO<sub>x</sub>/GaAs(100) interface using optical spin orientation. The effective value of the photocurrent asymmetry  $\Delta I_{\text{heli}}/2I_{\text{ph}}$  increases up to a maximum of 1.7% at a bias voltage of 0.04 V at room temperature. The effect is consistent with a model based on the tunneling transport across the AlO<sub>x</sub> layer inserted between the Fe and GaAs(100).

## ACKNOWLEDGMENTS

We are grateful to Professor H. Ahmed at Cavendish Laboratory for kindly offering the opportunity to use facilities at the Microelectronics Research Center. T. T. wishes to acknowledge the financial support of JSPS. G.W. would like to acknowledge the Austrian Academy of Sciences, the Wilhelm-Macke-Stipendienprivatstiftung (Austria), and the Cambridge Philosophical Society for their financial support. A.I. wishes to acknowledge Nordiko Ltd and the Cambridge European Trust for the financial support.

\*On leave from Department of Innovative and Engineered Materials, Tokyo Institute of Technology, Yokohama 226-8502, Japan. Electronic address: taniyama@iem.titech.ac.jp

†Electronic address: jacb1@phy.cam.ac.uk

<sup>1</sup>M. Johnson, *Science* **260**, 320 (1993).

<sup>2</sup>B.E. Kane, *Nature (London)* **393**, 133 (1998).

<sup>3</sup>H.J. Zhu, M. Ramsteiner, H. Kostial, M. Wassermeier, H.P. Schöenherr, and K.H. Ploog, *Phys. Rev. Lett.* **87**, 016601 (2001).

<sup>4</sup>V.P. LaBella, D.W. Bullock, Z. Ding, C. Emery, A. Venkatesan, W.F. Oliver, G.J. Salamo, P.M. Thibado, and M. Mortazavi, *Science* **292**, 1518 (2001).

<sup>5</sup>B.T. Jonker, Y.D. Park, B.R. Bennett, H.D. Cheong, G. Kioseoglou, and A. Petrou, *Phys. Rev. B* **62**, 8180 (2000).

<sup>6</sup>Y. Ohno, D.K. Young, B. Beschoten, F. Matsukura, H. Ohno, and D.D. Awschalom, *Nature (London)* **402**, 790 (1999).

<sup>7</sup>R. Fiederling, M. Keim, G. Reuscher, W. Ossau, G. Schmidt, A. Waag, and L.W. Molenkamp, *Nature (London)* **402**, 787 (1999).

<sup>8</sup>B.T. Jonker, A.T. Hanbicki, Y.D. Park, G. Itskos, M. Furis, G. Kioseoglou, A. Petrou, and X. Wei, *Appl. Phys. Lett.* **79**, 3098 (2001).

<sup>9</sup>A.T. Hanbicki, B.T. Jonker, G. Itskos, G. Kioseoglou, and A. Petrou, *Appl. Phys. Lett.* **80**, 1240 (2002).

<sup>10</sup>T. Manago and H. Akinaga, *Appl. Phys. Lett.* **81**, 694 (2002).

<sup>11</sup>V.F. Motsnyi, J.D. Boeck, J. Das, W.V. Roy, G. Borghs, E. Goovaerts, and V.I. Safarov, *Appl. Phys. Lett.* **81**, 265 (2002).

<sup>12</sup>M.W. Prins, H. van Kempen, H. van Leuken, R.A. de Groot, W.

van Roy, and J.D. Boeck, *J. Phys.: Condens. Matter* **7**, 9447 (1995).

<sup>13</sup>K. Nakajima, S.N. Okuno, and K. Inomata, *Jpn. J. Appl. Phys.* **37**, L919 (1998).

<sup>14</sup>A. Hirohata, J. Steinmueller, W.S. Cho, Y.B. Xu, C.M. Guertler, G. Wastlbauer, and J.A.C. Bland, *Phys. Rev. B* **66**, 035330 (2002).

<sup>15</sup>S.D. Ganichev, S.N. Danilov, V.V. Bel'kov, E.L. Ivchenko, M. Bichler, W. Wegscheider, D. Weiss, and W. Prettl, *Phys. Rev. Lett.* **88**, 057401 (2002).

<sup>16</sup>C. Cacho, Y. Lassailly, H.J. Drouhin, G. Lampel, and J. Peretti, *Phys. Rev. Lett.* **88**, 066601 (2002).

<sup>17</sup>D. Oberli, R. Burgermeister, S. Riesen, W. Weber, and H.C. Siegmann, *Phys. Rev. Lett.* **81**, 4228 (1998).

<sup>18</sup>S.F. Alvarado, *Phys. Rev. Lett.* **75**, 513 (1995).

<sup>19</sup>D.T. Pierce and F. Meier, *Phys. Rev. B* **13**, 5484 (1976).

<sup>20</sup>S. Yuasa, T. Sato, E. Tamura, Y. Suzuki, H. Yamamori, K. Ando, and T. Katayama, *Europhys. Lett.* **52**, 344 (2000).

<sup>21</sup>K.D. Choquette, M. Hong, H.S. Luftman, S.N.G. Chu, J.P. Mannaerts, R.C. Wetzel, and R.S. Freund, *J. Appl. Phys.* **73**, 2035 (1993).

<sup>22</sup>Y. Chye, V. Huard, M.E. White, and P.M. Petroff, *Appl. Phys. Lett.* **80**, 449 (2002).

<sup>23</sup>S. E. Andersenn, S. J. Steinmuller, A. Ionescu, C. M. Guertler, G. Wastlbauer, and J. A. C. Bland (unpublished).